

# We are IntechOpen, the world's leading publisher of Open Access books Built by scientists, for scientists

6,900

Open access books available

186,000

International authors and editors

200M

Downloads

Our authors are among the

154

Countries delivered to

TOP 1%

most cited scientists

12.2%

Contributors from top 500 universities



WEB OF SCIENCE™

Selection of our books indexed in the Book Citation Index  
in Web of Science™ Core Collection (BKCI)

Interested in publishing with us?  
Contact [book.department@intechopen.com](mailto:book.department@intechopen.com)

Numbers displayed above are based on latest data collected.  
For more information visit [www.intechopen.com](http://www.intechopen.com)



---

# Conducting Polymer Aerogels

---

Weina He and Xueting Zhang

Additional information is available at the end of the chapter

<http://dx.doi.org/10.5772/63397>

---

## Abstract

Conducting polymers are an important class of organic materials with electric conductivity and have experienced a rapid development. Meanwhile, as a novel class of porous nanomaterials, aerogels attract people's great interest for their ultra-low densities, large specific areas, rich open pores, etc. Thus, conducting polymer aerogels, combining the unique merits of aerogels with physicochemical properties relevant to conducting polymers, become a newly developed area. In this chapter, we give a brief introduction describing (1) synthesis strategies of conducting polymer (PEDOT, PPy, and PANi) aerogels through rational design for oxidant, cross-linker, soft template, sol-gel process, drying process; (2) advantages of these aerogels in physical and chemical performance, compared with the counterparts in bulk or membrane; and (3) their applications in energy storage, adsorption to metal-ions/dye-molecules, stress sensing, Joule heating. The chapter ends with a reflection on limitations of already proposed materials and a prospection of how conducting polymer aerogels developing in the future. As such, this chapter can act as a roadmap to guide researchers toward how conducting polymer aerogels produced and how these materials can be utilized, while also highlighting the current advancements in the field.

**Keywords:** conducting polymers, aerogel, sol-gel transition, energy storage, stress sensors

---

## 1. Introduction

### 1.1. Aerogels

"Aerogel" does not refer to a specific material with a set chemical formula but encompasses all materials with a specific geometrical structure, which is extremely porous with high

connectivity between nanometers-sized branched structures. The aerogel contains little solid and up to 99.8% volume of air; hence, it is often referred to as “frozen smoke.”

Aerogels, with merits of ultra-low densities, large specific areas, hierarchical open pores, elaborate 3D networks, etc., are a novel class of highly porous nanomaterials. These unique characteristics endow aerogels with interesting physical properties (low thermal conductivity, low sound velocity, etc.) and with potential applications (Cerenkov detectors, electronic devices, catalysis, etc.). The majority of aerogel is composed of silica, but carbon, metal, iron oxide, organic polymers, and semiconductor nanostructures can also form aerogels.

## 1.2. Conducting polymers

Intrinsically conducting polymers, also known as “synthetic metals,” are polymers with a highly conjugated polymeric chain. They have been studied extensively due to their intriguing electronic and redox properties, along with the resulting numerous potential applications in many fields since their discovery in 1970s. Typical conducting polymers include polyacetylene (PA), polyaniline (PANI), polypyrrole (PPy), polythiophene (PTh), poly(para-phenylene) (PPP), poly(phenylenevinylene) (PPV), polyfuran (PF), etc. The chemical structures of these polymers are illustrated in **Figure 1**.

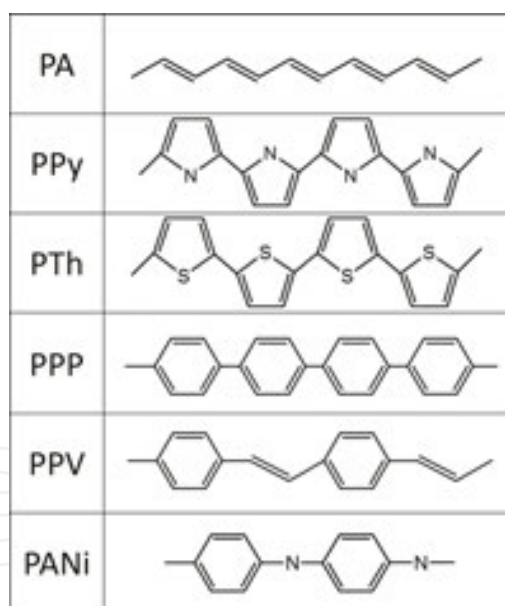


**Figure 1.** The chemical structures of typical conducting polymers.

These intrinsically conducting polymers exhibit adjustable electric conductivities, even across several orders of magnitude sometimes, depending on the level of doping or chemical/electrochemical treating. The reversibility of doping-dedoping endows these conducting polymer potential applications in actuators, sensors, etc., while the highly doped conducting polymers can be applied in nanoelectronic devices, corrosion protection coatings, microwave absorbing, etc., because of the high conductivity.

### 1.3. Conducting polymer aerogels

Aerogels can be divided into two categories according to their electrical properties: electric insulating aerogels and conducting ones. Conducting aerogels not only show ordinary properties as electric insulating aerogels but also exhibit excellent magnetic and electric-conducting performances. Therefore, conducting aerogels possess huge application potentials in energy storage, catalysis, sensing, electromagnetic shielding, and other fields. Heretofore, conductive aerogels are mainly obtained from (a) metal aerogel produced by sol-gel procedure, (b) carbonized product of organic aerogel, and (c) nanomaterial self-assembled by CNTs or G/GO sheets.

A new kind of conducting aerogels is produced by conducting polymers, named conducting polymer aerogels (CPAs). Theoretically, the inherent rigidity of most conducting polymers assist significantly in generating and maintaining permanent microporosity (pore diameter of  $<2$  nm). Through the nanostructural design, CPAs combine the individual superiorities of conducting polymers and aerogels, providing high surface area for more efficient separation and energy storage, more acting sites for fast functionalization with various guest objects, etc.

However, there are still lots of challenges remaining. At first, as a result of the fast oxidation and the poor solvent solubility of intrinsically conducting polymers, there are great difficulties in preparing CPAs in large scale by far. Secondly, because of the inherent rigidity of the conjugated macromolecular chains resulted from the delocalized  $\pi$ -electron system along the conducting polymer backbone, it needs to design particular structures and explores new preparing methods to make CPAs either strong or elastic. Fortunately, improvements in the fragility and brittleness of CPAs announced recently by Zhang's research group means that a whole new world of applications may be opened up in the future, from solid 3D conducting network to flexible electronics. To date, conducting aerogels can be made from poly(3,4-ethylenedioxythiophene) (PEDOT), polyaniline (PANi), polypyrrole (PPy) conducting polymers. The progress in CPAs will be summarized in this chapter to inspirit many new explorations surrounding conducting aerogels in the further.

## 2. Synthesis of conducting polymer aerogels

In general terms, aerogel is produced by the synthesis of gel precursors and drying process. At first, the gel is created in a solution as a precursor via sol-gel transition, and then, the liquid component is removed through drying process, which removes liquid skillfully in order to maintain the nanostructures.

### 2.1. Synthesis of gel precursors

PEDOT, PPy, and PANi can be easily synthesized by chemical oxidation coupling with the presence of a series of oxidants, such as  $(\text{NH}_4)_2\text{S}_2\text{O}_8$  (APS),  $\text{FeCl}_3$ ,  $\text{Fe}(\text{NO}_3)_3$ , and so on. However, because of the fast reaction rate of oxidation and the poor insolubility of the outcomes, the products often precipitated as granules. So as to obtain the intact hydrogels as the precursors

for aerogels, the oxidation rate should be controlled at first to let the reaction stop at the proper extent that the building blocks is neither too large to aggregated and separated as precipitates, nor too small to hardly support the framework or badly affect the electrical conductivity. The reaction rates are dependent on the concentration of monomers and oxidant or the reacting temperature. Thus, monomer suspension and oxidant solution with lower concentrations can be adopted, as well as lower reaction temperature provided by ice bath.

### 2.1.1. PEDOT gel

As for nonporous conducting polymers, the PEDOT:PSS (PSS is the abbreviation for poly(styrenesulfonate)) complex possess the merits of high dispersibility in water, excellent film-forming performance through conventional solution processing, and unique physical properties for the resulting films (high transparency in the visible range, high mechanical flexibility, and excellent thermal stability). So it becomes the most commonly used conducting polymer in commercial applications. Since PEDOT:PSS complex is highly soluble, it is most likely to realize the preparation of conducting aerogels.

As expected, it was reported by Zhang's group [1] that PEDOT-PSS supermolecular hydrogel could be obtained for first time by polymerizing 3,4-ethylenedioxythiophene (EDOT) with excess ferric nitrate as oxidizing agent in the presence of PSS. The PSS plays two general roles: (1) acting as the source for the charge-balancing counter-ion, and (2) keeping the EDOT segments dispersed in the sol. Compared with the nonporous PEDOT-PSS synthesis, the oxidant amount and reaction temperature have been controlled effectively during PEDOT-PSS hydrogel preparation.

The supermolecular cross-linking mechanism of the hydrogel precursors has also been discussed. If APS was used as oxidizing agent, there was no hydrogel formed. Additionally, it was revealed by X-ray photoelectron spectroscopy (XPS) that excess iron existed in PEDOT-PSS aerogel samples. Taken the two aspects into account, it could be deduced that the small amount of iron ions cross-link PSS to form three-dimensional networks driven by the electrostatic interaction between the metal ions and the anions attached to PSS.

Although PEDOT:PSS hydrogel have been prepared, the presence of insulating PSS inevitably inhibits the electrical properties of hydrogel. The synthesis of conducting polymer hydrogels (CPHs) as precursors for CPAs is still a great challenge due to the poor solubility of conducting polymers in aqueous solution, originating from the lack of hydrophilic groups and stiff chains. Hence, Zhang's group synthesize sodium 4-(2,3-dihydrothieno[3,4-b][1,4]dioxin-2-yl)-methoxybutane-1-sulfonate (EDOT-S), which is one of the thiophene derivatives used as an amphiphilic monomer (**Figure 2a**) [2].

Thus, they prepared CPHs in one step through a combination of oxidative coupling polymerization and non-covalent cross linking of the amphiphilic thiophene derivative (**Figure 2b**) [2]. APS is a well-known non-crosslinking oxidant that can polymerize aniline, pyrrole, EDOT, etc., via oxidative coupling, but the corresponding conducting polymers are in the form of a precipitate due to the stiffness of their backbones and strong  $\pi$ - $\pi$  interactions among large conjugated units in their backbones. Unsurprisingly, PEDOT-PSS gels cannot be obtained

oxidized only by APS. However, the conducting polymer hydrogel was obtained for the first time starting from the amphiphilic EDOT-S using only APS as the oxidant. This indicates that the introduction of the hydrophilic ionic group to the hydrophobic monomer plays a key role in the synthesis of CPHs, which provides electrostatic interactions of the ionized polymer chains as extra cross-linking sites. By contrast, when  $\text{FeCl}_3$  was used as the oxidant, the PEDOT-S hydrogels can be obtained under conditions of either a lower monomer concentration or a higher reaction temperature. This is probably due to the multivalent metal ions (excessive  $\text{Fe}^{3+}$ ) offering an additional cross-linking force to the sulfonate groups attached to PEDOT-S backbones. Moreover, when the mixture of APS and  $\text{FeCl}_3$  was used as the oxidant, a strikingly synergistic effect was achieved during synthesis.

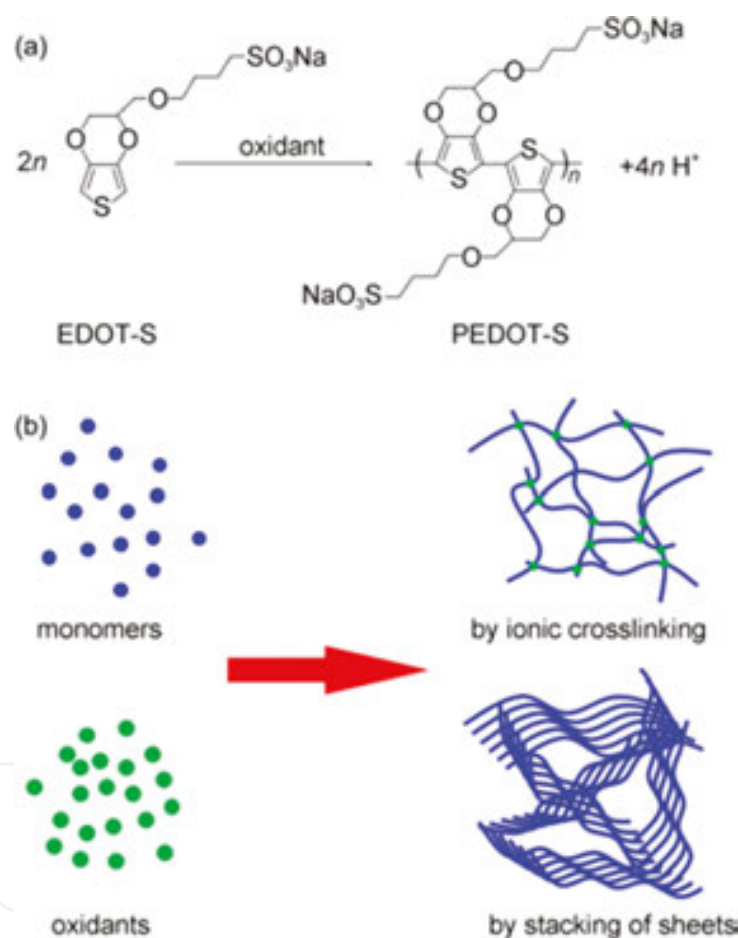


**Figure 2.** (a) Polymerization of EDOT-S into conducting polymer, and (b) schematic model for the formation of conducting polymer hydrogels through either ionic cross-linking or  $\pi$ - $\pi$  stacking. The oxidant used herein could be APS,  $\text{MCl}_3$ , or the mixture of them, where M represents Fe, La, Ce, Cr, or Sb [2].

Besides of the merits in gel forming, PEDOT-S can undergo significant 0D-2D transition during the polymerization and gelation process (**Figure 3**) [2]. The amphiphilic EDOT-S can self-assemble into sphere micelles in aqueous solution. However, when APS,  $\text{FeCl}_3$ , or APS- $\text{FeCl}_3$  was used as oxidant, PEDOT-S hydrogel was formed with the quasi-2D sheets, possessing an area-to-thickness ratio of much larger than 1000, serving as the building blocks.



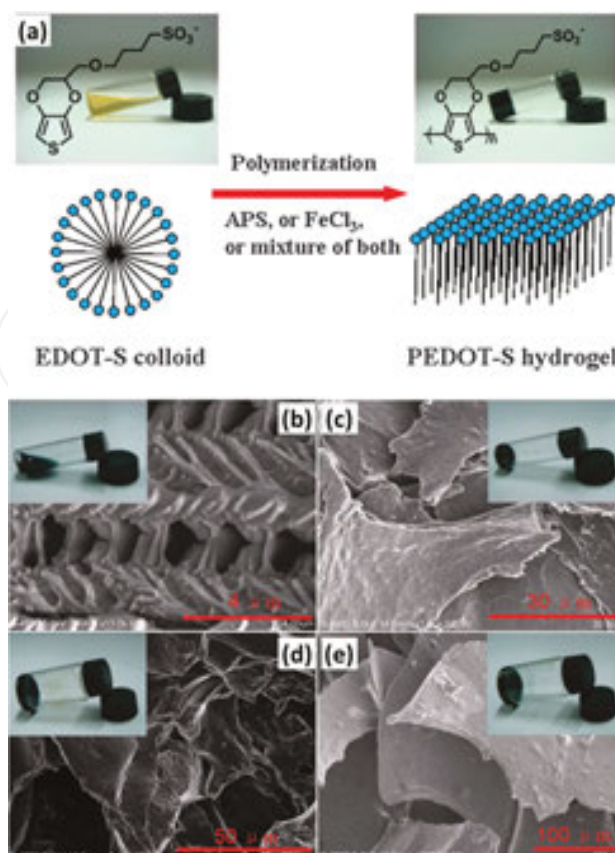


**Figure 3.** (a) A schematic diagram for synthesis of conducting polymer hydrogels. (b–e) SEM images of the resulting PEDOT-S products (see inset) synthesized with different oxidants: (b, c) using APS as the oxidant; (d) using FeCl<sub>3</sub> as the oxidant; (e) using a mixture of APS and FeCl<sub>3</sub> as the oxidant [2].

Considering the fact that the  $\pi$ - $\pi$  interactions are negligible unless the number of aromatic rings is three or more, the authors attributed the 0D-2D morphological transition to the gradually increased  $\pi$ - $\pi$  stacking effect. There is only one aromatic ring in each EDOT-S molecule, so the  $\pi$ - $\pi$  stacking can be neglected. Combined with the difficult-happened overlapping of ring planes of the monomers due to the steric hindrance, EDOT-S easily forms spherical micelles. However, with the process of polymerization, overlapping of the ring planes of the macromolecules easily occurs because of the increasing  $\pi$ - $\pi$  stacking among growing PEDOT-S macromolecules. Thus, initial EDOT-S spherical micelles gradually gather to form lamellar structure and ultimately convert into the PEDOT-S sheets.

Dimension evolution of the building blocks of the PEDOT-S hydrogel from 0D nanoparticles to 2D nanosheets did not only occur during polymerization and gelation process but was also observed by adjusting the reaction temperature or initial monomer concentration. It can be also explained by the enhanced  $\pi$ - $\pi$  interaction of the conjugated length of polymer, which could surpass the hydrophobic interaction in original spherical micelles [3].

Except for the 0D-2D morphological transition of building blocks, the PEDOT-s hydrogel also exhibits chemical potential-dependent gel-sol transitions [2]. Chemicals with standard electrode potentials higher than 0.8 V [APS, H<sub>2</sub>O<sub>2</sub>, K<sub>2</sub>Cr<sub>2</sub>O<sub>7</sub>, HNO<sub>3</sub>, Ce(SO<sub>4</sub>)<sub>2</sub>, etc.] triggered

disbanding of the resulting conducting polymer hydrogels (called over-oxidation mechanism which has been confirmed via UV spectroscopy), promoting the occurrence of gel-sol transitions. It was evidenced that the gel-sol transition was driven by the decrease of conjunction length in the delocalized  $\pi$  bond along the PEDOT-S chains caused by the strong oxidants.

Since EDOT-S can act as a reactive surfactant, it can be used to disperse EDOT to prepare PEDOT-S/PEDOT hydrogels through emulsion polymerization (**Figure 4**) [4]. The obtained hydrogels could also be an ideal precursor candidate for all-conducting polymer aerogels, which is the first all conducting polymer aerogel reported yet, with large BET surface areas, hierarchical pores, and abundant functional groups. It has been found that molar ratios of EDOT-S to EDOT have played a significant role in the stability of the EDOT-S stabilized EDOT emulsion – the higher molar ratio has led to the more stable colloid.

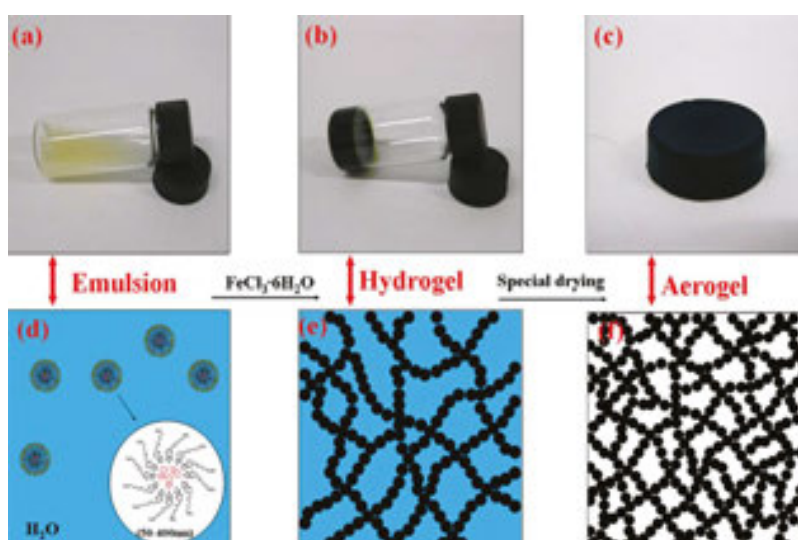


**Figure 4.** Emulsion-template synthesis strategy of all conducting polymer aerogels: digital photos of (a) EDOT emulsion stabilized by EDOT-S, (b) PEDOT-S/PEDOT hydrogel, (c) PEDOT-S/PEDOT aerogel and the corresponding schematic diagrams (d–f) [4].

### 2.1.2. PPy hydrogel

Hydrogel could not only be fabricated by PEDOT and their thiophene derivative, could also be prepared by PPy, and, what is more important, PPy hydrogel can exhibit high elasticity through two-step synthesis strategy.

On account of inherent rigidity of the conjugated macromolecular chains originated from the delocalized  $\pi$ -electron system along the polymer backbone, it has been a huge challenge to make conducting polymer hydrogels elastic. Hence, Zhang's group turned to the two-step synthesis method, which successively contains a fast and a slow reaction procedure, to prepare elastic PPy hydrogels (**Figure 5**) [5]. The fast reaction procedure contributes to the formation of incipient network with low joint density to show certain flexibility. The next slow reaction process strengthens the incipient framework by forming conformal polymer coatings. The two-



step synthesis method can be actualized by adopting deficient oxidant  $\text{Fe}(\text{NO}_3)_3$  ( $\text{Fe}^{3+}$  and  $\text{NO}_3^-$  dominate the fast and slow oxidation procedures, respectively) as oxidant and aging for 30 days.

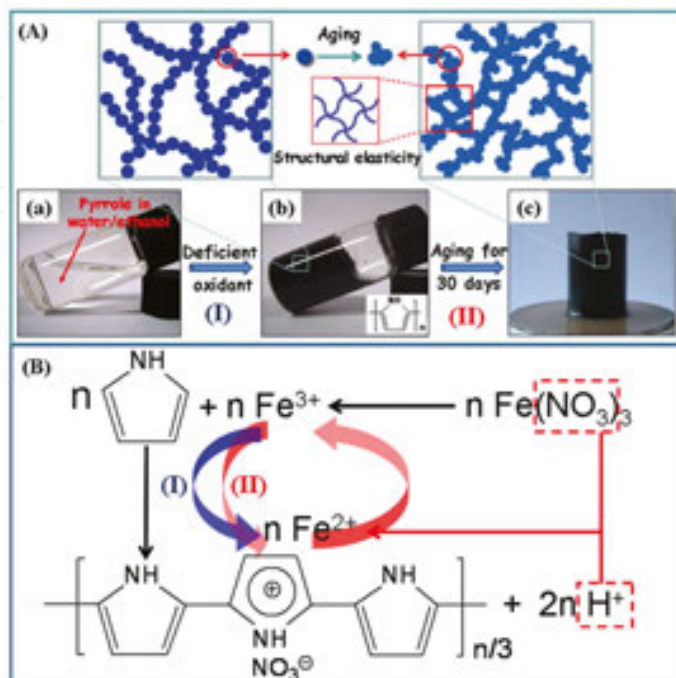


**Figure 5.** (A) The synthetic process of elastic polypyrrole hydrogel. Enlarged sketch maps indicated by squares in (A) have shown aggregated structural change of the polypyrrole hydrogel building blocks during polymerization. (B) The polymerization mechanism of the polypyrrole hydrogel [5].

To the best of our knowledge, it is the first report on the synthesis and properties of the elastic conducting polymer hydrogels. The work might also offer much inspiration to make more elastic conducting polymer hydrogels directly derived from PANi, PTh, etc., to prepare more elastic conducting aerogels.

### 2.1.3. PANi hydrogel

PANi hydrogels have been synthesized by embedding PANi into continuous matrix or using various non-conducting cross-linkers to cross-link PANi to form gels. However, both of the two strategies inevitably introduce non-conducting components, which impairs the performances of the resulting PANi hydrogels. Is it possible to make PANi hydrogels with continuous conjugated framework but without using any additional cross-linkers?

Herein self-cross-linked PANi hydrogels was synthesized for the first time via oxidative coupling reaction with APS as the oxidant and aniline hydrochloric salt as the precursor without any additional crosslinkers [6]. Aniline hydrochloric salt was chosen as the raw material on account of its water solubility and that the dissociated HCl could also dope PANi to ensure high conductivity. Aniline hydrochloric salt was oxidized by equimolar amount of

APS. With the polymerization proceeded, the PANi hydrogel formed. Subsequently, the hydrogel aged at ambient temperature to obtain an ideal precursor for PANi aerogels.

#### 2.1.4. Composite conducting hydrogels

Conducting hydrogels could be fabricated by typical conducting polymers (PEDOT, PPy, PANi) via well-designed synthesis strategies as maintained above. On this basis, conducting hydrogels can also composite with other functional materials to obtain more integrate performances for final aerogel products.

At first, by embedding carbon nanotubes into PEDOT-PSS supermolecular hydrogels in the presence of polyvinyl alcohol (PVA) as stabilizer for carbon nanotubes, Zhang's group [7] have prepared PEDOT-PSS/MWCNTs and PEDOT-PSS/c-MWCNTs composite gels with low densities of 0.04–0.07 g cm<sup>-3</sup>.

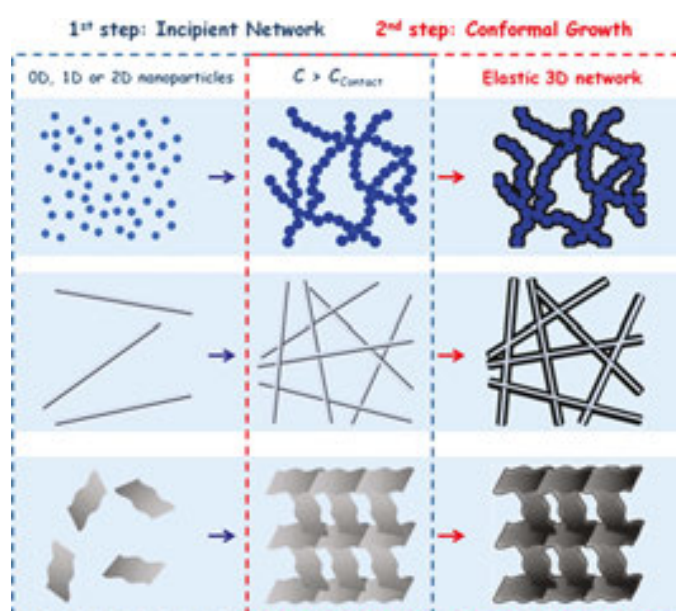


**Figure 6.** Schematic representation of incipient network conformal growth (INCG) technology [8].

On the basis of elastic PPy hydrogels, an incipient network conformal growth (INCG) technology was proposed to prepare hybrid and elastic porous materials (**Figure 6**) [8]. 0D, 1D, or 2D nanoparticles (NPs) are dispersed in solvent to form a uniform suspension at first. Once the concentration of suspension is within a proper range, the incipient network will form through NPs contacting with each other. The monomer of conducting polymer is then introduced and supposed to coating the incipient network conformally through polymerization. The conformal coatings not only endow NPs suspension with high dispersion but also offer composite conducting polymer with additional structural elasticity, meeting requirements for future generations of portable, compressive, and flexible devices.

To put INCG technology into practice, the fabrication process for PPy-Ag NW hybrid gels is demonstrated in **Figure 6** [8]. Ag nanowires (Ag NWs) were selected to contribute the incipient

3D networks considering easy synthesis and uniform diameters. Evaluated by Doi and Edwards theory, Ag NWs suspension with the volume fraction between  $\phi_1 = 8 \times 10^{-7}$  and  $\phi_2 = 10^{-3}$  was appropriate to form an incipient 3D networks. Above  $\phi_1 = 8 \times 10^{-7}$ , the dispersed Ag NWs in suspension began to contact with each other. Pyrrole (Py) was then added and preferentially adsorbed to the surface of Ag NWs resulting from metal- $\pi$  strong interactions, to form core-shell structures. Once the oxidant was introduced in the next, Py was oxidized and polymerized in situ. Thus, the 3D network and the core-shell morphology were fixed, obtaining PPy-Ag NW coaxial nanowire aerogels.

Besides, a “wet” process to incorporate chiral polyaniline nanowires into the agarose was put forward, and hence, the chiroptical properties could be attached to PANi hydrogels [9]. The chiral polyaniline nanofibers were obtained by successively using potassium tetrachloroaurate (PTC) and APS to oxidize aniline in the presence of (1S)-(+)-10-camphorsulfonic acid [(S)-(+)-CSA] or (R)-(-)-CSA as a chiral-inducing agent. The optical activity of the chiral polyaniline is dependent on the mass ratio of PTC to APS, reaching peak values in the ratio range of 1.0–2.5. The chiroptical properties of the polyaniline nanofibers are retained within the composite hydrogel, although the degree of chiral organization of the polyaniline appears to be somewhat modified by the presence of the agarose matrix.

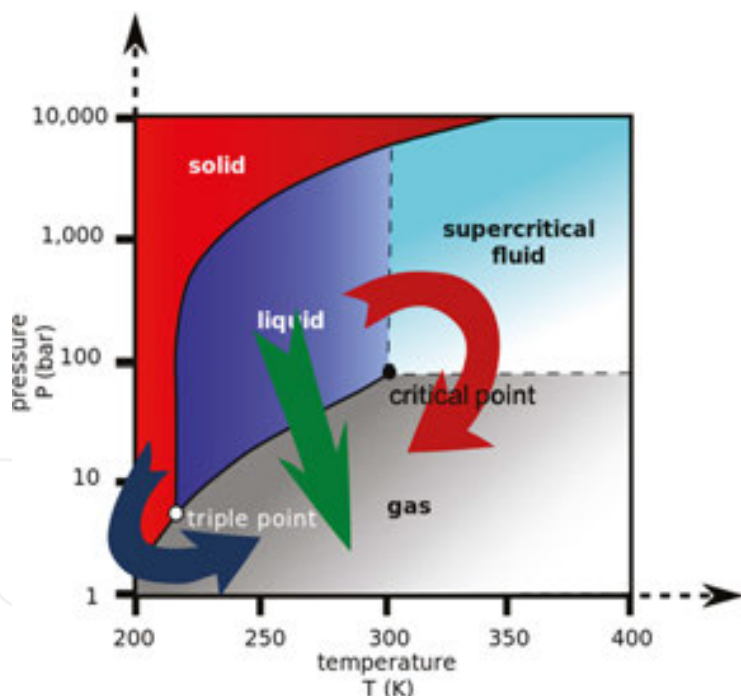


**Figure 7.** Phase diagram of pure materials and arrow illustrations of different drying process (supercritical drying—red arrow, ordinary drying—green arrow, and freeze-drying—blue arrow).

## 2.2. Drying of gel precursors

After the conducting polymer hydrogels were produced, the hydrogels should be processed into aerogels by replacing the liquid solvent with air. When a substance is dried via normal

methods of applying heat and pressure at a finite rate, the substance passes through the liquid-gas barrier (green arrow in **Figure 7**), where the amount of capillary stress changes, causing the substance to deflate. To avoid this problem, there are supercritical drying (SCD), which dries a substance via high heat and pressure and goes beyond the critical point (red arrow in **Figure 7**), and freeze-drying, which goes through solid-gas barrier (blue arrow in **Figure 7**) to avoid the direct liquid-gas transition.

### 2.2.1. Supercritical drying

Supercritical drying (SCD) is performed to replace the liquid in a material with a gas to isolate the solid component without destroying the material's delicate nanostructured porous network. Carbon dioxide ( $\text{CO}_2$ ) is the most used as supercritical fluid, because it is supercritically extracted at a lower temperature ( $31.1^\circ\text{C}$ ) than an organic solvent without the risk of combustion. Through low-temperature SCD, most of the obtained conducting polymer hydrogels mentioned above, such as PEDOT-PSS, PEDOT-s/PEDOT, PEDOT-PSS/MWCNTs, PPy, PPy/Ag NW, PANi hydrogels, can be converted into corresponding aerogels successfully. Low-temperature supercritical drying for aerogel production conducts as follows:

A gel is prepared using sol-gel chemistry. The gel contains a mixture of organic solvent and water in its pores.

1. The gel is soaked in a pure organic solvent (ethanol, methanol, acetone, amyl acetate, etc.) and changes the solvent for several times over several days to remove the original solvent from its pores.
2. Finally, the gel is supercritically dried in a pressure vessel. The gel is placed in a pressure vessel, and the pressure vessel is then filled with liquid  $\text{CO}_2$ . Adjusting temperature and pressure to make the gel soaked in supercritical  $\text{CO}_2$  and flushing through new  $\text{CO}_2$  every 1–2 h. After the solvent in the pores of the gel has been completely replaced by supercritical  $\text{CO}_2$ , the vessel is then isothermally depressurized to give aerogels.

It is notable that when the solvent of the gel is exchanged for supercritical  $\text{CO}_2$ , the gel may also shrink slightly. This stems from favorable interactions between the two liquids, to put it simply, molecules take up smaller space in a mixture than molecules in either of the separate liquids. Solvents with low volume changes of mixing with supercritical  $\text{CO}_2$  include acetone, amyl acetate, ethanol, and methanol. In general, aerogels made using supercritical drying from  $\text{CO}_2$  may shrink up to 5%. Even so, low temperature SCD is still the best drying method to maintain deliberate nanostructures of aerogels so far.

### 2.2.2. Freeze-drying

Although SCD is a mostly used drying method to maintain deliberate nanostructures of aerogels, it is not always successful for gel precursors, because (1) some conducting polymer gels dissolve in alcohol or acetone, like aforementioned PEDOT-s hydrogels [2, 3], (2) gels are prepared in solvent which cannot exchange with alcohol or acetone or supercritical  $\text{CO}_2$  and (3) some metal-containing gels will react with the carbon dioxide to create metal carbonates.

In these circumstances, the freeze-drying is a common alternative for gel precursors to proceed into aerogels (also called cryogels sometimes).

In freeze-drying, the gel precursors were usually quickly frozen in liquid  $N_2$  at first. Then, reduce the surrounding pressure to allow the frozen solvent in the gel pores to sublime directly from the solid phase to the gas phase, leaving aerogels.

To avoid the structural damages caused by ice crystals of solvent produced and grown during the freezing process, the frozen process should finish within the shortest time, usually quenching the gel precursors in liquid  $N_2$  with a very quick speed. Well, it is indeed a crazy idea to carry out in a diametrically opposite way, called ice-segregation-induced self-assembly (ISISA) [10]. The pore morphology of resulting cryogels can be well controlled via ISISA process by unidirectional freezing at a definite immersion rate (**Figure 8**). During unidirectional freezing, crystalline ices are produced, causing the original dispersed solute to be expelled to the boundaries between adjacent ice crystals gradually. After experiencing freeze-drying, the ordered-arranged solutes become “walls,” enclosing the empty spaces that formerly occupied by ice crystals. Aligned or unaligned conducting polymer cryogels with 3D macroporous architectures have been prepared using the ice-segregation-induced self-assembly (ISISA) of different PEDOT-PSS freezing precursors as a dispersion or a formed hydrogel.

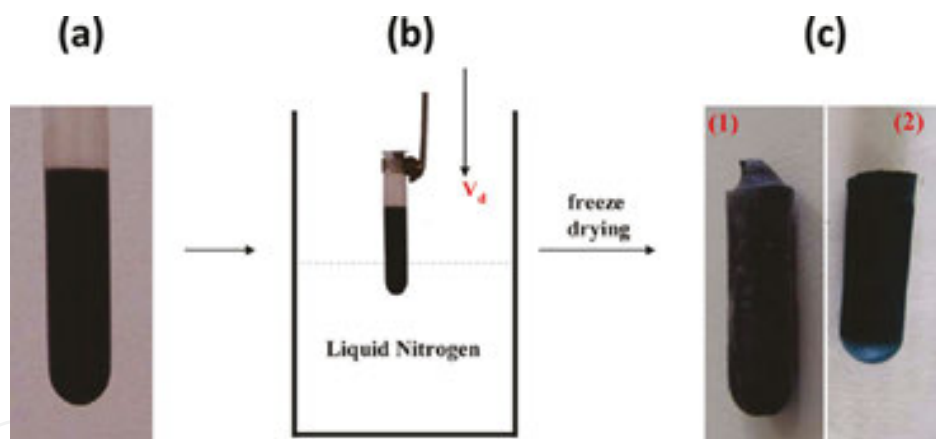


**Figure 8.** (a) An example of the PEDOT-PSS freezing precursor held in a plastic centrifugal tube. (b) A schematic diagram for unidirectional freezing of the PEDOT-PSS precursor by dipping vertically into liquid nitrogen at a rate of 3–50  $\text{mm min}^{-1}$ . (c) Digital photos of the PEDOT-PSS cryogels starting from dispersion (left) and hydrogel (right) [10].

It is believed that ISISA is a facile method for producing hierarchically macroporous 3D monoliths of conducting polymers with many advantages as follows. (1) It is a green and inexpensive method for ice template was merely needed without any other organic solvents. (2) It is facile, reproducible, and readily controllable by adjusting immersion rate, solute concentration, etc. (3) It endows conducting polymers with unusual long-range ordered macropores, which may introduce many unexpected properties and thus may exploit some new applications in the fields of electronic components (including batteries and transistors, solar cells), tissue engineering, and next-generation catalytic and separation supports.



### 3. Properties of conducting polymer aerogels

#### 3.1. PEDOT aerogels

The PEDOT-PSS aerogels dried through SCD show low density ( $0.138\text{--}0.232\text{ g cm}^{-3}$ ), large surface area ( $170\text{--}370\text{ m}^2\text{ g}^{-1}$ ), and hierarchical porous structures [1]. The resulting PEDOT-PSS aerogel (with molar ratio of 1:1 for PEDOT: PSS) has a conductivity of  $10^{-1}\text{ S cm}^{-1}$ , being comparable with the value of PEDOT-PSS thin film.

Processing PEDOT-PSS via ISISA endows the conducting polymers with novel properties. Well-ordered alignment of the macroporous structure could be observed along the longitudinal direction (i.e., the ice growth direction) for the resulting aerogels from SEM, which resulted from phase separation that occurs during the directional freezing process (**Figure 9**) [10]. Closer observations in different areas showed that there were several domains with random orientations over the whole macroporous monolith and that the boundaries of these domains could be easily recognized. More interestingly, unexpected fingerprint-like morphology can be observed from the cross section of the cone-shaped bottom of the cryogel (**Figure 9d**). This may be attributed to the super-cooling of the dispersion in the immersed portion, thus instead of crystalline ice, the amorphous ice grow and act as a template. These observations may indicate an efficient way to produce the man-made fingerprint for identifications and markings.

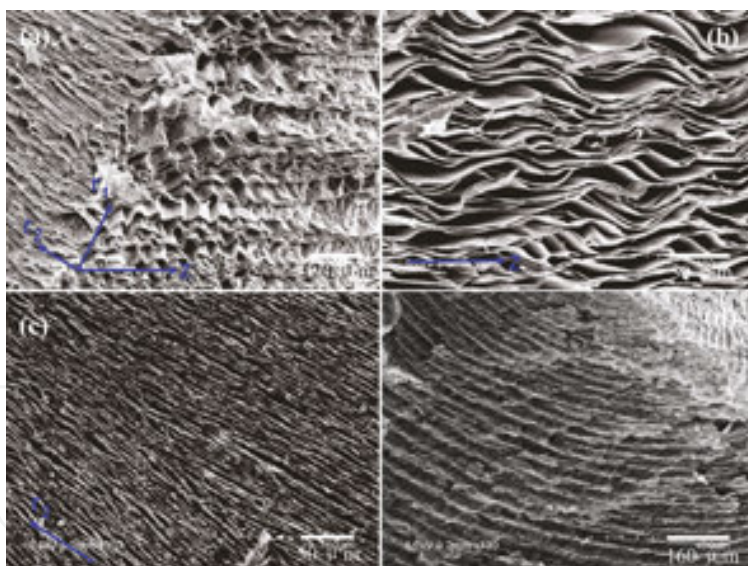


**Figure 9.** SEM images of PEDOT-PSS cryogel prepared via ISISA showing a well-ordered macropore structures from (a) the whole domain, (b) face  $Zr_1$ , (c) face  $r_1r_2$ , and (d) cross section of the cone-shaped bottom of the cryogel. (Arrow Z and r denotes the longitudinal and radial directions,  $Z \perp r_1 \perp r_2$ .) [10].

Besides, all conducting polymer PEDOT-S/PEDOT aerogels obtained by emulsion polymerization and dried through SCD have high conductivity with the level of  $10^1\text{ S m}^{-1}$  [4]. In comparison with any other conventional aerogels, the resulting PEDOT-S/PEDOT aerogels, without the necessity of further functionalization, show superb adsorption ability to various guest substances, such as dyestuffs and heavy metal ions, and enhanced electrochemical.

Furthermore, the specific surface areas, thermal stability, and electrical conductivities can be significantly enhanced by embedding MWCNTs into PEDOT-PSS aerogel matrix [7]. The resulting composite aerogels show low density ( $0.044\text{--}0.062\text{ g cm}^{-3}$ ), large surface area ( $280\text{--}400\text{ m}^2\text{ g}^{-1}$ ), high electrical conductivity ( $1.2\text{--}6.9 \times 10^{-2}\text{ S cm}^{-1}$ ), and hierarchical porous structures.

### 3.2. PPy aerogels

The PPy hydrogel could be also readily converted into the lightweight, elastic, conductive, and aerogel through SCD. Thus, pure organic, electrically conductive (ca.  $0.5\text{ S m}^{-1}$ ), lightweight ( $0.07\text{ g cm}^{-3}$ ) PPy aerogel was first obtained by Zhang's group (**Figure 10**) [5]. The obtained aerogels have still kept the excellent elasticity after drying of the PPy hydrogels, which could be compressed by  $\geq 70\%$  and recovered to its original shape in 30 s.

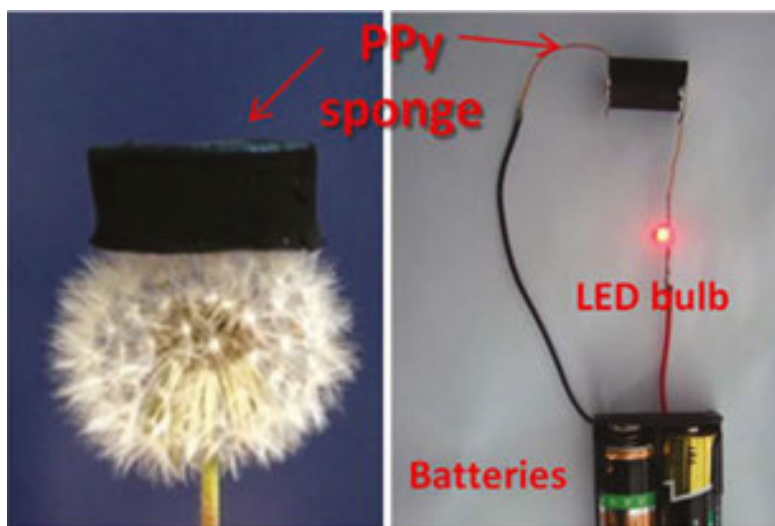


**Figure 10.** Digital photos of the lightweight, elastic, conductive, and organic PPy aerogels made from the resulting PPy hydrogels through supercritical fluid drying process located on a dandelion and connected to the LED bulb [5].

The authors attributed the elasticity of the PPy aerogels to the elaborate synthesis design and the resulting micro-structural changes. (1) At first, the reaction rate is slowed down and the reaction extent is limited by adopting the deficient oxidant, bringing an incipient network with the reduced joint density. Thus, the obtained PPy aerogels exhibit less stiffness. (2) Then, the initial network can be reinforced effectively by coarsening the framework conjunctions, benefited from the secondary growth during the slow reaction process. Thus, the obtained PPy aerogels can avoid the structural fracture when suffering compressions. (3) At last, the asymmetrically epitaxial growth of the original polymer particles during the secondary growth offers many new weak contacting joints. Single-point contacting for the building blocks of traditional PPy aerogels suffering compression is replaced by multi-point contacting or even face contacting. Thus, inside stress of the compressed PPy aerogels can be easily dissipated, preventing damage caused by stress concentration. In summary, the PPy aerogels can restrict the irreversible fracture of the hydrogel network when bearing compression.

Besides PPy aerogels, PPy-Ag NW aerogels prepared through INCG [8] also exhibited superb compressive elasticity, which could be compressed by large deformations (>90%) and return to its original shape in seconds once withdrawing the compression (**Figure 11a, b**). From the comparison stress-strain ( $\sigma$ - $\epsilon$ ) curves for 50 compress-release circles along the loading direction with under a fixed max strain of 20%, PPy-Ag NW aerogel recovered their deformations with little mechanical failures (**Figure 11c**).

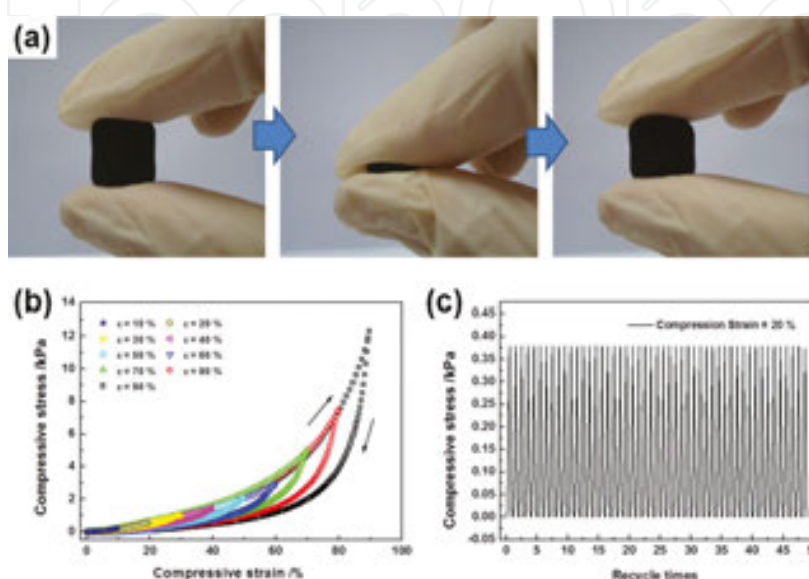


**Figure 11.** (a) Digital pictures showing a superb elasticity of PPy-Ag NW aerogel. (b)  $\sigma$ - $\epsilon$  curves for PPy-Ag NW aerogel along the loading direction during loading-unloading cycles ( $\epsilon = 10$ –90%). (c) 50 consecutive compression tests for PPy-Ag NW aerogel at  $\epsilon = 20\%$  [8].

Similarly to PPy aerogels, the superb elasticity of PPy-Ag NW aerogels also comes from the rational-designed nanostructures. The resultant PPy-Ag NW aerogels possess: (1) strong and flexible 3D network contributed by ultra-long coaxial nanowires, giving aerogels resistance and elasticity to external compressions by bending their framework skeletons; (2) rich pores, making aerogels possible to dissipate the external compressive energy by shutting off the pores; (3) in situ welded junctions and strong metal- $\pi$  interactions, avoiding the interfacial slippage resulting from the poor load transfer between adjacent coaxial nanowires or Ag NW and PPy coatings.

### 3.3. PANi aerogels

Self-cross-linked PANi hydrogels can be also converted to corresponding aerogels by SCD [6]. The obtained aerogels exhibit adjustable densities from 0.03–0.15 g cm<sup>-3</sup>, coral-like micro-morphology, high BET surface area (39.54 m<sup>2</sup> g<sup>-1</sup>), and comparative mechanical strength. The resulting PANi aerogels showed a coral-like micro-morphology, formed by branched nanofibers with a diameter of 50–150 nm and a length up to tens of micrometers (**Figure 12**). This unique morphology insures higher electrochemical performance, because the charges can transport effectively in 3D porous network than the corresponding bulk materials.

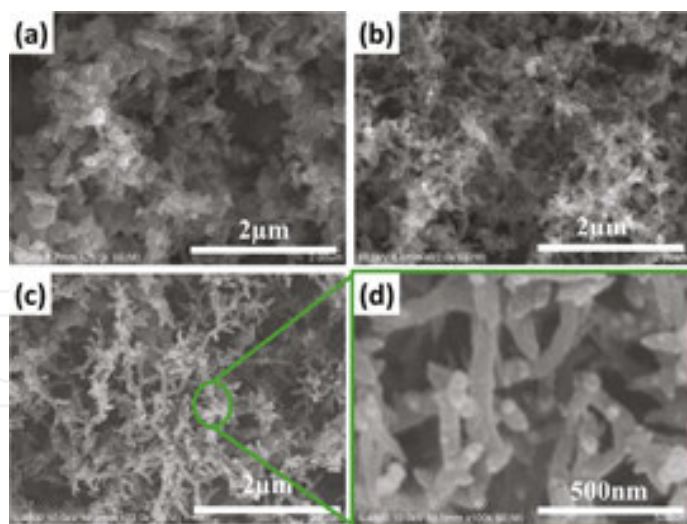


**Figure 12.** SEM images of PANi hydrogels with a density of (a)  $0.05 \text{ g cm}^{-3}$ , (b)  $0.08 \text{ g cm}^{-3}$ , (c)  $0.11 \text{ g cm}^{-3}$ , and (D) the magnified image of PANi hydrogel with  $0.11 \text{ g cm}^{-3}$  [6].

As the obtained PANi aerogels exhibit high porosity from SEM detections, it is necessary to analysis their specific surface area and pore size distribution (PSD) by Brunauer-Emmett-Teller (BET) tests. The adsorption-desorption isotherm curve (**Figure 13**) of PANi aerogels presents the characteristic feature of the type-IV isotherm with a H3 hysteresis loop, indicating the existence of a large number of mesoporous (with a diameter of 2–50 nm). A further analysis shows that PANi aerogel possesses a BET specific surface area of  $39.54 \text{ m}^2 \text{ g}^{-1}$  and a unimodal pore size distribution peak around 28 nm. The high surface area and mesoporous structure are supposed to enlarge electrode-electrolyte contact surface and boost the electrolyte transfer obviously.

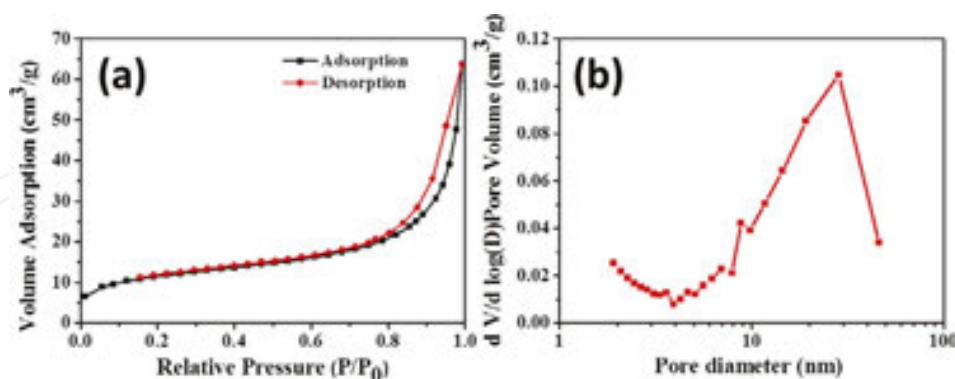


**Figure 13.** (a) Nitrogen adsorption/desorption isotherms of PANi aerogels analyzed by BET detections and (b) the corresponding pore size distribution [6].

Besides, PANi aerogels exhibit increasing mechanical strength with the increase of the PANi density. The comparative mechanical strength insures better integrity of the hydrogel network, which also contributes to better transfer of ions, charges, and electrons in redox reaction interface during electrochemical tests.



## 4. Application of conducting polymer aerogels

The large surface area and wide pore size distribution, together with their electro properties, would allow these conducting polymer aerogels to be applied in many fields with unexpected performance.

### 4.1. Electrochemical energy storage

The conducting polymer hydrogels and aerogels show superior electro-chemical properties including a fast electrochemical response, a high specific capacitance, and a low electric resistance, resulting from the combined merits of organic semiconductors and three-dimensional porous gels.

At first, the electrochemical capacitive behavior of the supercritically dried PEDOT-S/PEDOT aerogel has been investigated by cyclic voltammetry (CV) between 0.2 and 0.6 V in 1.0 mol L<sup>-1</sup> KCl solution [4]. Fixing the scan rate at 50 mV s<sup>-1</sup>, the CV curves for both PEDOT-S/PEDOT and PSS/PEDOT aerogel electrodes show a rectangular-like shape with an obvious wide peak at the potential interval of -0.2 to 0.0 V, indicating the presence of a pseudo-capacitive effect caused by the redox of the conducting polymers. The electrochemical capacitance of the electrode materials can be calculated further from the integral CV area. For the PEDOTS/PEDOT aerogel, the electrochemical capacitance is 68.5 F g<sup>-1</sup>, much more than the value of the PSS/PEDOT aerogel electrode (19.2 F g<sup>-1</sup>). Furthermore, the good rate capability (slight decay of the electrochemical capacitance along with the increase of the scan rate) and high cycling stability (negligible changes of the electrochemical capacitance after 100th charge-discharge cycle) of the resulting PEDOT-S/PEDOT aerogel electrode have been further confirmed from CV detections. The excellent performance in electrochemical energy storage of the resulting PEDOT-S/PEDOT aerogel electrode might be ascribed to low ionic resistance and fast kinetics of the electrochemical process in an aqueous medium.

In the meanwhile, CV curves of the PEDOT-S gels were recorded in 1.0 mol L<sup>-1</sup> Na<sub>2</sub>SO<sub>4</sub> aqueous solution [3]. The specific capacitance of the PEDOT-S hydrogels is estimated to be ca. 30–60 F g<sup>-1</sup>, which is much higher than PEDOT:PSS gels. This can be ascribed to the higher proportion of active ingredients in PEDOT-S than PEDOT:PSS gels for PSS does not contribute electrochemical capacitance directly.

Besides PEDOT aerogels, PANi gels are proved to be a promising material for electrochemical energy storage [6]. For the self-cross-linking PANi hydrogel, functionalized electrodes have exhibited a new record of specific capacitance (750 F g<sup>-1</sup>). At first, CV curves of the PANi hydrogel electrode were collected in 1.0 M H<sub>2</sub>SO<sub>4</sub> electrolyte solution (**Figure 14**). The representative redox peaks, which belong to the transformation between leucoemeraldine base (LB), emeraldine salt (ES), and pernigraniline base (PB), persisted from 5 to 200 mV s<sup>-1</sup>, indicating a high stability in redox electrochemical activity. Then, EIS analysis was performed to evaluate the charge transfer property of PANi hydrogel. The solution resistance of the PANi gel electrode is as low as 1.7 X. The charge-transfer resistance of electrode of the PANi hydrogel electrode is <0.1 X, which is remarkably low due to well-matched resistance between the PANi



hydrogel (electronic conductivity) and liquid electrolyte phase (ionic conductivity), insuring good ion transport within 3D gel framework. At last, chronopotentiometry (CP) tests were carried out to further evaluate the electrochemical energy storage performance of PANi hydrogel electrode (**Figure 14**). 75.8% capacitance remained with the increasing current density from  $2 \text{ A g}^{-1}$  ( $588 \text{ F g}^{-1}$ ) to  $20 \text{ A g}^{-1}$  ( $446 \text{ F g}^{-1}$ ), indicating an excellent rate capability for high power performance. The specific capacitance of the PANi hydrogel electrodes is dependent on hydrogel density, reaching the peak level ( $750 \text{ F g}^{-1}$ ) at the density of  $0.11 \text{ g cm}^{-3}$ .

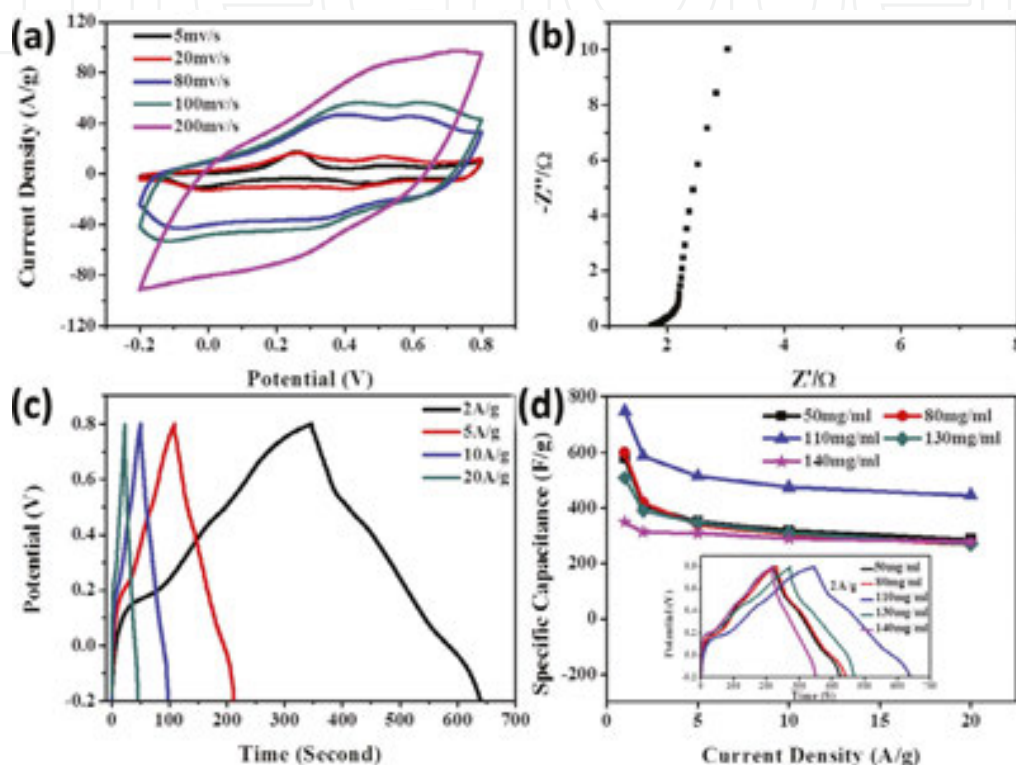


**Figure 14.** Electrochemical performance of PANi hydrogel electrodes: (a) cyclic voltammogram curves, (b) Nyquist plot, (c) galvanostatic charge/discharge curves, (d) specific capacitances of PANi hydrogel electrodes with various PANi densities, and (d-inset) chronopotentiogram curves of PANi hydrogel electrodes at current density of  $2 \text{ A g}^{-1}$  [6].

## 4.2. Stress sensing

Piezoresistive sensors, transducing pressure message to resistance signal, have been rapidly developed and widely used for their advantages in high sensitivity, fast response, feasible fabrication, low cost, and easy signal collection. Conductive and elastic aerogels are an emerging kind of candidates for fabrication of piezoresistive sensors because of their combinational electric conductivities and mechanical flexibilities.

As mentioned above, the PPy hydrogel can be readily converted into the lightweight, elastic, conductive, and organic aerogels via SCD [5]. The obtained aerogels have still kept the excellent elasticity after drying of the PPy hydrogels and been made into stress sensors successfully. The decreases of the electrical resistance are directly proportional to the compression strain,

reaching at 3% when the aerogel was compressed by 80%. It is not difficult to understand that the external responses in electrical properties are brought by the different contacting situations of the gel network upon compressive stresses. The resistance decreases of the compressed PPy aerogels could complete within 1.5 s and so was the electrical resistance returns to the original value once being released. It is because of the elasticity of PPy aerogels that their gel skeletons can bend and recover in seconds without structural fractures. Besides of the short response time, the electrical responses of PPy aerogels also exhibit high stability under compress and release circles.

Although pure conducting polymer aerogels show great potentials in stress sensing, they have not solved the “temperature drift,” a common problem that the piezoresistive materials always meet caused by the temperature-dependent electrical resistances. Hence, self-temperature compensated sensors are highly desirable in direct and precise measurement. The most feasible solution is developing hybrid sensing materials with a low/nearly zero temperature coefficient resistivity (TCR) by offsetting the positive and negative temperature dependence of electric resistance. In this respect, the polypyrrole/silver (PPy/Ag) coaxial nanowire hybrid aerogel prepared via INCG [8] is a wise choice for Ag NWs show positive temperature-coefficient, while PPy show negative temperature-coefficient. Through the reasonable selection of the ratio of Ag NWs at 83.3%, the electric resistance of the hybrid aerogels can be immune from temperature influence, showing a nearly zero temperature coefficient (**Figure 15a**).

To process into a stress sensor, PPy-Ag NW aerogel was imbedded into two parallel copper electrodes, as shown in **Figure 15b**. The electric resistance decreased directly with the compression strain, changing by 83% at the strain of 80% (**Figure 15d**). The electric resistance response of PPy-Ag NW aerogel caused by compression could be completed within 1 ms and so was the electric resistance recovery after compression released. The detection minimum was as low as 4.93 Pa when the aerogel was compressed by 0.5%. Furthermore, the electrical response of PPy aerogel upon stress exhibited high stability, indicated by suffering hundreds of compression-release circles for each compressive strain (**Figure 15e**). The sensitivity  $S (= \delta(\Delta R/R_0)/\delta\sigma)$  was as high as  $0.33 \text{ kPa}^{-1}$  for the nearly zero temperature coefficient sample, while  $S = 0.06 \text{ kPa}^{-1}$  for another sample with a Ag NW content of 2.7 wt% (**Figure 15f**). It implies that a series of sensing samples with different sensitivities can be prepared by programmed synthesis to meet the needs of applications. There was no deviation in sensing performance at different temperatures (15, 25°C) (**Figure 15f**) or after 3 V electric heating for 160 s, affirming the high sensing stability of the PPy-Ag NW aerogel sensor with nearly zero temperature coefficient.

### 4.3. Joule heating

A stress-triggered Joule heater can be fabricated by aerogels used for stress sensing in principle. Under compression, the electric resistance can be reduced and the Joule heating generated by electric current running through aerogels can be raised. It is possible that the thermal generation may be inconspicuous for aerogels in original state upon inputting a proper voltage, while for the compressed aerogels, the Joule heating can raise its temperature considerably, named stress-triggered Joule heating.

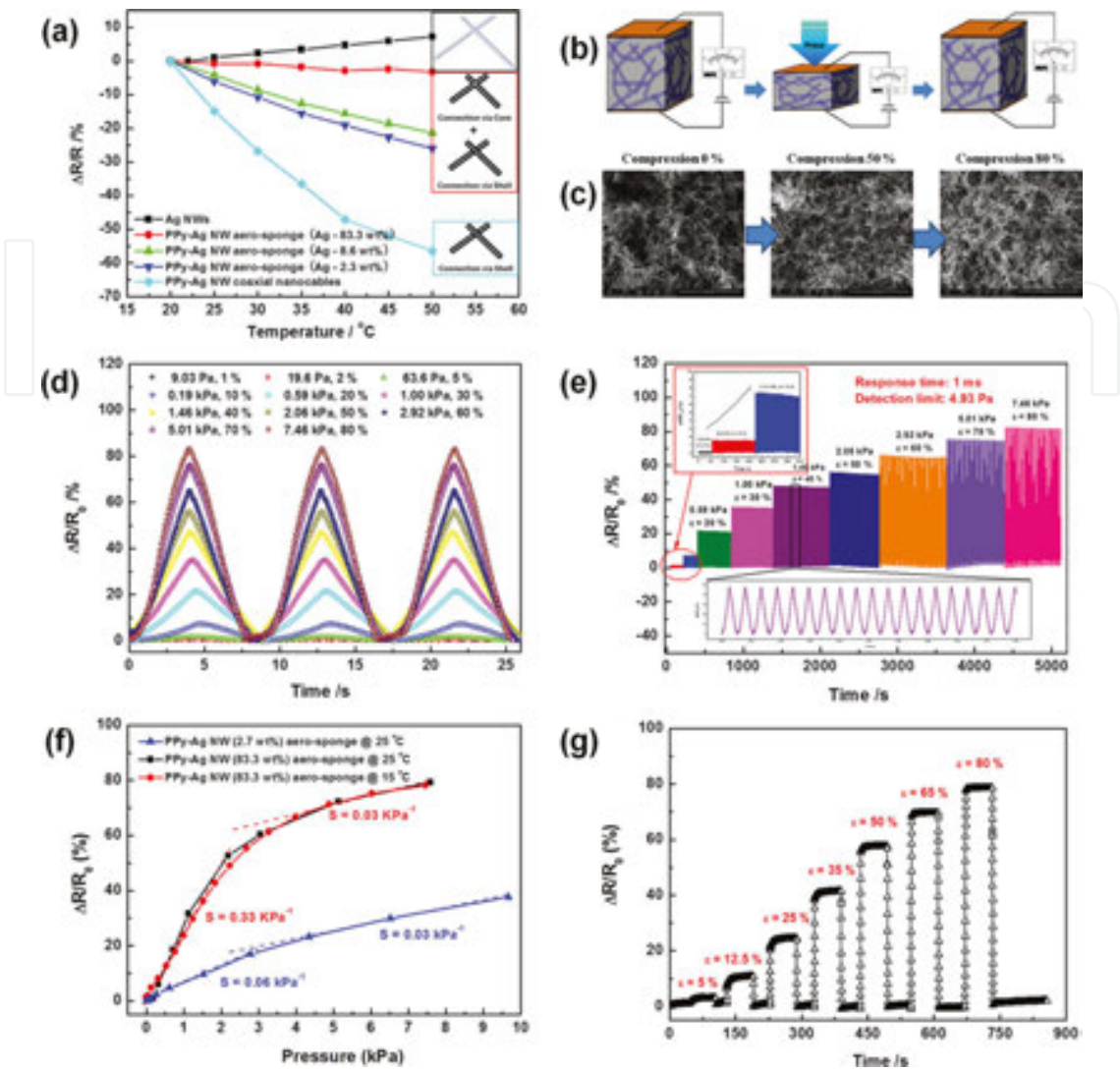


**Figure 15.** Performance of PPy-Ag NW hybrid aerogels in stress sensing. (a) Curves of how the electric resistance changes with temperature relatively ( $\Delta R/R \sim T$ ) for Ag NWs, PPy-Ag NW membrane deposited by nanocable suspension, and PPy-Ag NW hybrid aerogel, respectively. (b) Schematic illustration of how to prepare a stress sensor with PPy-Ag NW aerogel. (c) SEM images of PPy-Ag NW aerogel with compression. (d) Multiple-cycles electric resistance tests under a series of repeated loading-unloading pressures with 1 V input. (e) Reliability test of PPy-Ag NW hybrid aerogel under a series of repeated loading-unloading pressures with partial enlarged details in insets. (f) Comparison of how electric resistance changes with compressive pressure relatively ( $\Delta R/R \sim p$ ) for the nearly zero temperature coefficient PPy-Ag NW aerogel performed at 25 and 15°C. (g) Electric resistance response of the nearly zero temperature coefficient PPy-Ag NW aerogel at different strains by introducing a series of persistent compressive pressure [8].

The stress-triggered Joule heater can be fabricated by PPy-Ag NW hybrid aerogel, which is placed on thermal insulating blanket and covered by a reversible thermo-allochroic membrane (**Figure 16a**) [8]. Inputting a persistent voltage of 3 V, the Joule heating generated by electric current running through the original aerogel was mostly dissipated and will not causing any visible differences for thermo-allochroic membrane (**Figure 16b**). However, if imposing a persistent compressive pressure, the electric current was boosted by nearly four times. As a consequence, Joule heating increased, warmed the aerogel, and induced the color

changes of the thermo-allochroic membrane (the temperature point of color transition for thermo-allochroic membrane used in this work is about 43°C) (**Figure 16c**). Once the compressive pressure was released, the membrane returned its original color gradually, indicating the temperature recovery of the aerogel.

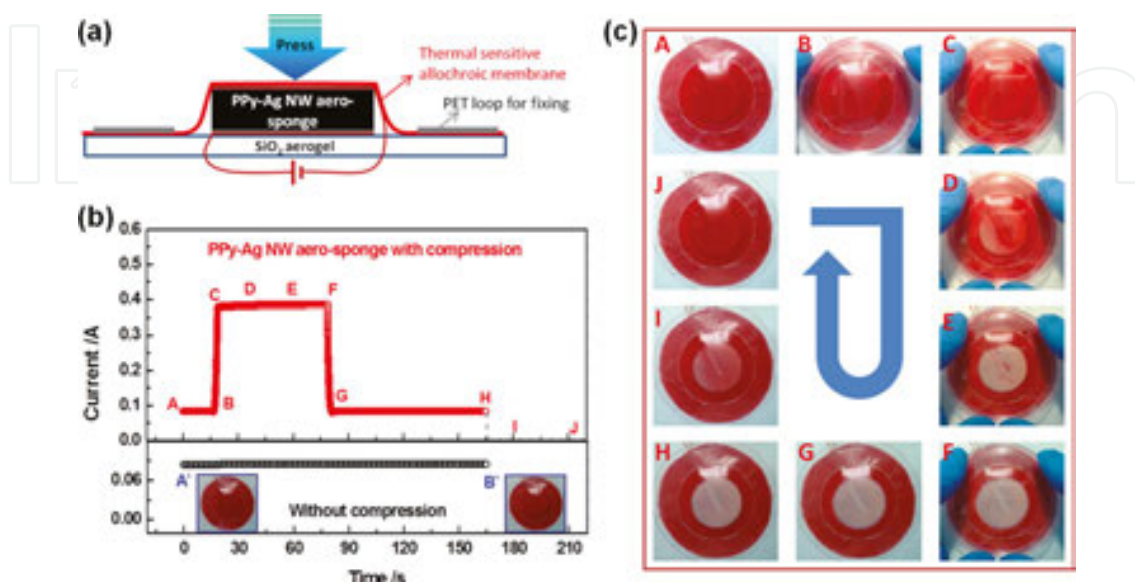


**Figure 16.** The performance of stress-triggered Joule heater. (a) Schematic illustration of how to construct a stress-triggered Joule heater with PPy-Ag NW aerogel. (b) Real-time I–t curves of the stress-triggered Joule heater under both free and compressive states with 3 V voltage input, and inset is the digital pictures of the Joule heater in free state. (c) Digital pictures of the intelligent Joule heater at the corresponding time point marked in (b) [8].

#### 4.4. Adsorbing and separation

Hierarchical pores, a large surface area, and abundant conjugated chain or functional groups have endowed the conducting polymer aerogels with adsorption ability of some guest substances, such as heavy metals, dye molecules, etc.

For PEDOT aerogels, let us have a look at molecular structure of PEDOT-S at first. The conducting polymers possess linear  $\pi$ -conjugated system and lots of attached sulfonic acid groups. The  $\pi$ -conjugated system makes both of PEDOT-S and PEDOT-S/PEDOT aerogels show good affinity to the most of  $\pi$ -conjugated based dyestuffs via  $\pi$ - $\pi$  stacking. But the adsorptive capacities of these aerogels to cationic and anionic dyestuffs exhibit a significant difference, contributed by the electrostatic interaction of the adsorbed dyestuffs and the sulfonic acid groups attached on the PEDOT-S polymer chains. The adsorptive capacity of PEDOT-s and PEDOT-S/PEDOT aerogels can reach around 164 and 170 mg g<sup>-1</sup> for basic fuchsin, while gels can only adsorb 39 and 160 mg g<sup>-1</sup> acid fuchsin, respectively [3, 4]. Moreover, for both of the two kinds of aerogels, the adsorbed basic fuchsin can be released by addition of a cationic surfactant cetyltrimethyl ammonium bromide (CTAB) and the more the CTAB added, the more the basic fuchsin released, which provides an efficient way to control the release of the adsorbed dye molecules.



In addition, the PEDOT-S/PEDOT aerogel also show certain adsorptive capacity to heavy metals ions caused by electrostatic interactions [4]. But the adsorptive capacity is not uniform towards different kind of metals, 184.1 mg g<sup>-1</sup> for Hg<sup>2+</sup>, 111.1 mg g<sup>-1</sup> for Ag<sup>+</sup>, 79.6 mg g<sup>-1</sup> for Pb<sup>2+</sup>, and 28.3 mg g<sup>-1</sup> for Cu<sup>2+</sup>. Author ascribed it to the different affinity of metal ions to alkoxy sulfonate groups attached on the main chains of the conducting polymer. On all accounts, these adsorption investigations have shown a very promising application of the PEDOT aerogels in the removal of color and heavy metal ions from wastewater, etc.

Although there is no ionized functional group attached on PPy chains, the  $\pi$ -conjugated structures can provide enough active sites for dyestuff adsorptions. The high specific surface area (ca. 12 m<sup>2</sup> g<sup>-1</sup>), excellent mechanical strength, and strong  $\pi$ - $\pi$  interaction between dye molecules and sorbent matrix allow PPy aerogels to extract dye molecules from the dye solutions in a very fast and effective way (**Figure 17**) [5].

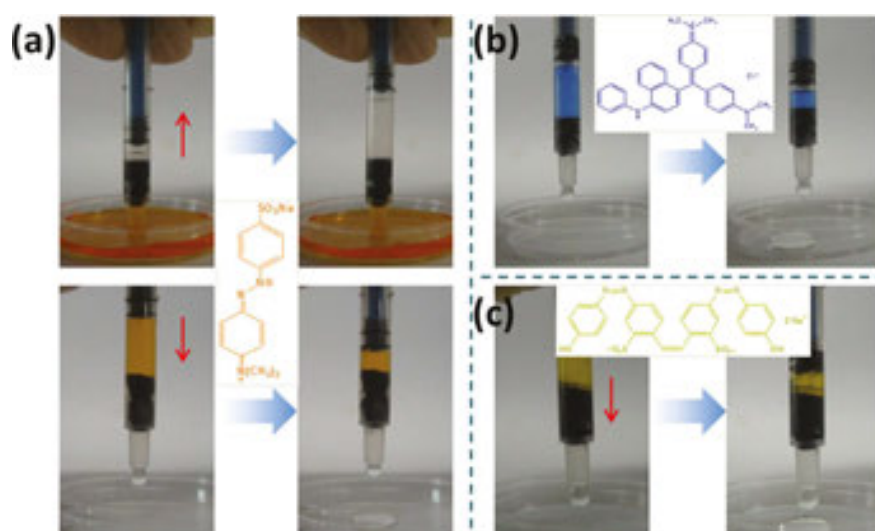


**Figure 17.** Digital photos showing fast removal of (a) methyl orange, (b) victoria blue, and (c) brilliant yellow from waste water with the elastic PPy hydrogels in syringes [5].

The PPy gels were placed in the tube of a syringe, and the plunger was pulled or pushed allowing take in or expel the dye solutions after permeating through the PPy hydrogels. For all three kinds of dye molecules, the colorful dye solutions changed into colorless in several seconds. PPy gel could absorb methyl orange (MO) with a capacity of 389.5 mg g<sup>-1</sup> and an efficiency of 99.99%. Besides, the used hydrogel can be refreshed by treating with NaOH aqueous solution with a concentration of 2 mol L<sup>-1</sup> at 80°C, and the refreshed gel could still adsorb MO with a capacity of 196.4 mg g<sup>-1</sup> and an efficiency of 99.89%.

## 5. Outlook: problems, prospects, and challenges

This chapter has focused on recent research progress in the development of conducting polymer aerogels, with specific focus on PEDOT-containing, PPy, and PANi aerogels discus-



sing from (1) synthesis strategy of conducting polymer (PEDOT, PPy, and PANi) aerogels through rational design for oxidant, cross-linker, soft template, sol-gel process, drying process; (2) advantages of these aerogels in physical and chemical performance, compared with the counterparts in bulk or membrane; and (3) applications in energy storage, adsorption to metal-ions/dye-molecules, stress sensing, Joule heating.

However, there are still lots of challenges remaining. At first, as a result of the fast oxidation and the poor solvent solubility of intrinsically conducting polymers, there are great difficulties in preparing conducting polymer aerogels in large-scale by far. Secondly, because of the common existing differences in physicochemical properties, it lacks universal methods to make widely used conducting polymer aerogels. Besides, lots of the exploited applications of conducting polymer aerogels in the present go back to the liquid surroundings, such as electrochemical energy storage, dyestuff absorption, liquid-phase catalysis, etc., making drying process futile to some extent.

As such, the future development of conducting polymer aerogels will focus on (1) exploring new universally applicable synthesis strategies on the base of INCG, emulsion polymerization, two-step synthesis, ISISA described in this chapter; (2) expanding new application areas of conducting polymer aerogels, especially applications in gas environment, such as gas phase catalysis, air purification, solar cells, electrostatic shielding, heat insulation combining with thermoelectric conversion functions, etc. Enlightened by the progress of typical PEDOT, PPy, and PANi aerogels presented in this chapter, we expect to witness the widespread use of many new conducting aerogels in the near future.

## Acknowledgements

The authors would like to thank the financial supports from National Natural Science Foundation of China (21504104) and the Natural Science Foundation of Jiangsu Province (BK20140391).

## Author details

Weina He<sup>1</sup> and Xuotong Zhang<sup>2,3\*</sup>

\*Address all correspondence to: [xtzhang2013@sinano.ac.cn](mailto:xtzhang2013@sinano.ac.cn)

1 Shanghai Jiao Tong University School of Medicine, Shanghai, People's Republic of China

2 Suzhou Institute of Nano-tech and Nano-bionics, Suzhou, People's Republic of China

3 Beijing Institute of Technology, Chinese Academy, Beijing, People's Republic of China

## References

- [1] Zhang X.T., Chang D.W., Liu J.R., Yunjun Luo Y.J. Conducting polymer aerogels from supercritical CO<sub>2</sub> drying PEDOT-PSS hydrogels. *Journal of Materials Chemistry*. 2010;20(24):5080–5085. doi:10.1039/c0jm00050g
- [2] Du R., Xu Y.Z., Luo Y.J., Zhang X.T., Zhang J. Synthesis of conducting polymer hydrogels with 2D building blocks and their potential-dependent gel–sol transitions. *Chemical Communications*. 2011;47(22):6287–6289. doi:10.1039/c1cc10915d
- [3] Du R., Zhang X.T. Alkoxysulfonate-functionalized Poly(3,4-ethylenedioxythiophene) hydrogels. *Acta Physico-Chimica Sinica*. 2012;28(10):2305–2314. doi:10.3866/PKU.WHXB201209142
- [4] Xu Y.Z., Sui Z.Y., Xu B., Duan H., Zhang X.T. Emulsion template synthesis of all conducting polymer aerogels with superb adsorption capacity and enhanced electrochemical capacitance. *Journal of Materials Chemistry*. 2012;22(17):8579–8584. doi:10.1039/c2jm30565h
- [5] Lu Y., He W.N., Cao T., Guo H.T., Zhang Y.Y., Li Q.W., et al. Elastic, conductive, polymeric hydrogels and s. *Scientific Reports*. 2014;4:5792. doi:10.1038/srep05792
- [6] Guo H.T., He W.N., Lu Y., Zhang X.T. Self-crosslinked polyaniline hydrogel electrodes for electrochemical energy storage. *Carbon*. 2015;92:133–141. doi:10.1016/j.carbon.2015.03.062
- [7] Zhang X.T., Liu J.R., Xu B., Su Y.F., Luo Y.J. Ultralight conducting polymer/carbon nanotube composite aerogels. *Carbon*. 2011;49(6):1884–1893. doi:10.1016/j.carbon.2011.01.011
- [8] He W.N., Li G.Y., Zhang S.Q., Wei Y., Wang J., Li Q.W., et al. Polypyrrole/silver coaxial nanowire aero-sponges for temperature-independent stress sensing and stress-triggered Joule heating. *ACS Nano*. 2015;9(4):4244–4251. doi:10.1021/acs.nano.5b00626
- [9] Zhang X.T., Chechik V., Smith D.K., Walton P.H., Duhme-Klair A.K., Luo Y.J. Nano-composite hydrogels-controlled synthesis of chiral polyaniline nanofibers and their inclusion in agarose. *Synthetic Metals*. 2009;159(19–20):2135–2140. doi:10.1016/j.synthmet.2009.08.002
- [10] Zhang X.T., Li C.Y., Luo Y.J. Aligned/unaligned conducting polymer cryogels with three-dimensional macroporous architectures from Ice-Segregation-Induced Self-Assembly of PEDOT-PSS. *Langmuir*. 2011;27(5):1915–1923. doi:10.1021/la1044333